The Effects of Glaucoma on the Pressure-Induced Strain Response of the Human Lamina Cribrosa

Dan Midgett*¹, Baiyun Liu¹, Yik Tung Tracy Ling¹, Joan L. Jefferys², Harry A. Quigley², and Thao. D. Nguyen^{1,3}

¹Department of Mechanical Engineering, The Johns Hopkins University, Baltimore, MD 21218, USA
²Wilmer Ophthalmological Institute, School of Medicine, The Johns Hopkins University, Baltimore, MD 21287, USA
³Department of Materials Science, The Johns Hopkins University, Baltimore, MD 21218, USA

Abstract

Purpose. To measure the *ex-vivo* pressure-induced strain response of the human optic nerve head and analyze for variations with glaucoma diagnosis and optic nerve axon damage.

Methods. The posterior sclera of 16 eyes from 8 diagnosed glaucoma donors and 10 eyes from 6 donors with no history of glaucoma were inflation tested between 5-45mmHg. The optic nerve from each donor was examined for degree of axon loss. The posterior volume of the lamina cribrosa (LC) was imaged with second harmonic generation (SHG) and analyzed using volume correlation to calculate LC strains between 5-10 and 5-45mmHg.

Results. Eye length and LC area were larger in eyes diagnosed with glaucoma ($p \le 0.03$). Nasal-temporal E_{XX} and circumferential $E_{\theta\theta}$ strains were lower in the LC of diagnosed glaucoma eyes at 10mmHg ($p \le 0.05$) and 45mmHg ($p \le 0.07$). E_{XX} was smaller in the LC of glaucoma eyes with < 25% axon loss compared to undamaged normal eyes (p = 0.01, 45 mmHg). In general, the strains were larger in the peripheral than central LC. The ratio of the maximum principal strain E_{max} in the peripheral to central LC was larger in glaucoma eyes with >25% axon loss than in glaucoma eyes with milder damage (p = 0.004, 10mmHg).

Conclusions. The stiffness of the LC pressure-strain response was greater in diagnosed glaucoma eyes and varied with glaucomatous axon damage. Lower LC strains in glaucoma eyes with milder damage may represent baseline biomechanical behavior that contributes to axon loss, while greater LC strain and altered radial LC strain variation in glaucoma eyes with more severe damage may be caused by glaucoma-related remodeling.

Pages: 17, Word Count: 5886, Tables: 13, Figures: 8

Keywords: glaucoma, lamina cribrosa, optic nerve head, biomechanics, intraocular pressure *Supported by:* NSF CAREER Award 1253453, PHS Grants EY021500, EY02120, and EY01765; Brightfocus Foundation grant G2015132; National Science Foundation Grant CMMI-1727104; and the Microscopy and Imaging Core Module, Wilmer Core Grant for Vision Research.

^{*} Corresponding Author, Email: dan.midgett@yale.edu

1 Introduction

Glaucoma is a neurodegenerative disease characterized by the dysfunction and death of retinal ganglion cell (RGC) axons at the lamina cribrosa (LC) in the optic nerve head (ONH). This is accompanied by significant remodeling of the connective tissue structure of the LC, which gives the optic disk in advanced glaucoma patients a more excavated appearance ??. The level of intraocular pressure (IOP) is an important risk factor that correlates with the prevalence of glaucoma and the severity of glaucomatous axon damage ??. IOP acts to deform the tissues of the ONH by imposing a translaminar pressure difference and inducing tensile hoop stresses in the adjacent sclera. The LC is the main load-bearing tissue structure of the ONH that serves to support the RGC axons as they pass from the intraocular space into the optic nerve. The collagen beams of the LC also house mechanosensitive astrocytes, fibroblast-like cells called lamina cribrocytes, and microglia, 10 as well as nourishing capillaries?. The biomechanical response of the LC to IOP fluctuations may regulate 11 the homoeostasis in the ONH ??. Changes in the structure and mechanical properties of the LC may alter the mechanical and physiological support of the RCG axons and contribute to the susceptibility and severity of glaucomatous axon damage. Variations in the LC structure and stiffness may explain why some ocular 14 hypertensives do not develop glaucoma while others with normal or low IOP develop glaucoma. 15

Advances in volumetric imaging methods, such as optical coherence tomography (OCT) and multiphoton 16 microscropy, and volume correlation methods have enabled direct, spatially-resolved measurements of ONH 17 deformation in response to changes in IOP in human ??????, mouse ?? and porcine eye ?, and to changes 18 in IOP and intracranial pressure (ICP) in monkey eyes ??. Midgett et al. ? developed an ex vivo inflation test that used second harmonic generation (SHG) imaging of collagen in the posterior LC volume and digital 20 volume correlation (DVC) to measure the strain response of the human LC to controlled pressurization. LC 21 strains were larger in the peripheral LC compared to the central LC. Comparing the nasal, temporal, inferior, 22 and superior LC quadrants, maximum principal strain was lowest in the nasal quadrant. Specimen-averaged maximum principal strain also decreased significantly with age, suggesting a structural stiffening with age. Behkam et al. ? developed a different inflation test that also used SHG volume imaging and DVC to measure the pressure-strain response of the human LC and compared for differences between different racioethnic groups. They found significant differences in the shear strains and regional variation of the strain

components in the LC between Hispanic, African-derived and European-derived racial groups. Girard et al. ? used OCT to image the visible anterior portion of the ONH in patients before and after trabeculectomy 29 and applied DVC to calculate strain relief after the IOP-lowering surgery. Beotra et al. ? applied the same 30 methods to measure LC strains following acute IOP elevation by an ophthalmodynamometer in healthy, 31 ocular hypertensive, and glaucoma subjects. Effective LC strain in subjects with ocular hypertension was 32 significantly smaller than in healthy subjects, but was not significantly different compared to glaucoma 33 subjects. There were also no significant differences in LC strain between patients with primary open angle glaucoma (POAG) and angle closure glaucoma (ACG). These studies have highlighted average differences 35 in the LC pressure-strain response of glaucoma eyes, but so far no study has examined how regional strain 36 distribution within the LC differs between glaucoma and healthy eyes and with the degree of axonal damage. The objective of this study is to measure the IOP-induced deformation of the LC in post-mortem normal 38 and glaucoma donor eyes and analyze for variations with glaucoma diagnosis and optic nerve axon damage. The ex vivo inflation test method developed by Midgett et al. ? was applied to measure strains in the LC between the pressures of 5-10 mmHg and 5-45 mmHg. LC strains were analyzed for regional variations and the effect of LC area.

43 2 Methods

The specimen preparation, SHG imaging, DVC algorithm and strain calculation methods were described previously in Midgett et al. ?. The following section briefly summarizes these methods and the methods used for RGC axonal loss grading, LC area calculation, and statistical analysis of the effects of glaucoma diagnosis, degree of axonal damage, and variations with LC region and area.

48 2.1 Eye tissues

Ten eyes from 6 donors with no prior history of glaucoma (Table ??) and 16 eyes from 8 donors diagnosed with glaucoma (Table ??) were obtained from the National Disease Research Interchange (NDRI), Eversight, and the Minnesota Lions Eye Bank within 24 hours *post-mortem* and subjected to inflation testing within 48 hours *post-mortem*. All donors were of Caucasian descent and there were equal numbers of male and

female donors. The normal and glaucoma groups had the same age range, 76-93 years and a similar average age, 83.8 ± 6.1 years and 87.3 ± 5.4 years respectively. Glaucoma eyes were confirmed based on retrieved medical records and/or confirmation of previous glaucoma diagnosis by family members. Five of 8 glaucoma donors were diagnosed with POAG, one donor had chronic ACG, one donor had pseudoexfoliation glaucoma, and one had an unknown glaucoma type. Medical records for the 16 glaucoma eyes indicated the last IOP measurement for 14 eyes, the cup to disk ratio for 7 eyes, and visual field measurements for 6 eyes (Table \ref{Table}).

Glaucoma diagnosis was provided by written material submitted by the institutions providing the post 60 mortem eyes. In some cases, there was minimal information other than the diagnosis and the fact that typical glaucoma eye drop medication was used pre-mortem. In other cases, some eye examination notes were available. In order to categorize the degree of axonal damage in glaucoma eyes, a masked, qualitative 63 evaluation of axon loss in the optic nerve cross-sections in epoxy-embedded, thick sections was made. Optic nerve sections were excised from the eye for all specimens 1-3 mm posterior to the LC, fixed in a 4% paraformaldehyde solution, embedded in epoxy resin, and sectioned into 1 μ m thick slices. A glaucoma specialist (HQ), masked to the diagnosis, examined the sections and assigned a grade for the degree of axon 67 loss, as shown in prior studies ????? (Table ??-??). The assigned grades were 10% or less loss, 10%-25% loss, 25%-50% loss, 50%-75% loss, and 75% or more loss. In the normal group, the optic nerve of 8 of 10 eyes had an appearance of 10% or less loss, 1 had 10%-25% loss, and 1 had 25%-50% loss. Of the 16 eyes in the glaucoma group, the optic nerve of 6 eyes had an appearance of 10% or less loss, 3 had 10%-25% loss, 71 3 had 25%-50% loss, 3 had 50%-75% loss, and 1 did not have enough optic nerve to obtain an adequate section for grading (unknown). No eyes had 75% or more loss. On masked re-grading, the grading of 3 nerves changed between the 10% or less and the 10%-25% loss categories. In this study, we have therefore divided the diagnosed glaucoma eyes to only 2 groups, those with 25% or less axon loss (GM) and those with greater than 25% axon (GS). The normal eyes are divided into undamaged (NU) with 10% or less axon loss and damaged (ND) with >10% damage. It should be noted that Eye 16 with pseudoexfoliation (PEX) glaucoma had 10% or less axon damage, while the PEX glaucoma eye 15 from the same donor had 25%-50% axon damage. PEX glaucoma can often presented unilaterally, thus Eye 16 may have been misdiagnosed as a glaucoma eye. Eyes 17 and 18 had an unknown glaucoma diagnosis. The history of glaucoma treatment

Eye ID	Age(yr)	Sex	Side	optic nerve damage
1	88	M	Left	ND
2*	90+	F	Left	NU
3*	90+	F	Right	NU
4*	79	M	Right	NU
5*	79	M	Left	NU
6	76	M	Right	NU
7*	83	F	Right	ND
8*	83	F	Left	NU
9*	84	F	Right	NU
10*	84	F	Left	NU

Table 1: Donor information for eyes with no glaucoma history. * Indicates left and right eyes from the same donor. The categories NU indicate 10% or less optic axon loss and ND indicate >10% optic axon loss in masked, qualitative analysis of optic nerve thick sections embedded in epoxy.

- of these eyes was equal to the other eyes, but the specific type of glaucoma was not determinable from the
- available clinical record. The optic nerves also had 10% or less axon damage, thus Eyes 17 and 18 also may
- have been misdiagnosed as having glaucoma.

84 2.2 Specimen preparation

The eye length of eyes 4-26 was measured with calipers as the distance from the center of the cornea to the opposing posterior surface of the globe, just superior to where the optic nerve protruded. The extraocular tissues were removed from the donor eyes, and the optic nerve was excised 1 mm posterior to the scleral surface to avoid cutting into the LC. Multiple thin cuts were made to remove the myelinated posterior lamina tissue and expose the trabecular structure of the LC. The specimen was examined under a dissecting microscope after each cut to confirm the exposure of the LC. The eye was glued (Permabond 910, Electron Microscopy Sciences, Hat- field PA) to a custom polycarbonate ring 3-5 mm anterior to the equator, such that the ONH was centered in the ring. The cornea and anterior sclera were excised from the eye and the intraocular components, including the retina and choroid, were removed leaving only the posterior scleral shell. The posterior scleral specimen was kept hydrated in a 1 M phosphate-buffered saline (PBS) throughout specimen preparation and inflation testing.

Eye	Age (yr)	Sex	Side	Diagnosis	Last IOP	Visual Field	Cup-to-disk	optic nerve damage
11*	90+	M	Right	POAG	15	-9.37 dB	0.7	GS
12*	90+	M	Left	POAG	15	-6.29 dB	0.45	GM
13*	90+	F	Right	ACG	12	98% VFI	0.5	GM
14*	90+	F	Left	ACG	11	60% VFI	0.6	GS
15*	86	M	Right	Pseudoexfoliation	14	_	_	GS
16*‡	86	M	Left	Pseudoexfoliation	14	_	_	GM
17*‡	89	M	Right	Unknown	_	_	_	GM
18*‡	89	M	Left	Unknown	_	_	_	GM
19*	76	M	Right	POAG	22	_	_	GM
20*	76	M	Left	POAG	27	_	_	GM
21*	85	F	Right	POAG	13	_	_	GS
22*	85	F	Left	POAG	13	_	_	GS
23*	90+	F	Right	POAG	16	-1.8 dB	0.8	GM
24*	90+	F	Left	POAG	16	-3.1 dB	0.8	GM
25*	86	F	Right	POAG	13	_	0.5	GS
26*	86	F	Left	POAG	13	_	_	Unknown

Table 2: Donor information for eyes diagnosed with glaucoma. * Indicates left and right eyes from the same donor, and ‡ indicates that the glaucoma diagnosis may be uncertain. The categories GM indicate 25% or less optic axon loss and GS indicate >25% optic axon loss in masked, qualitative analysis of optic nerve thick sections embedded in epoxy.

96 2.3 Imaging

Posterior scleral cup specimens were mounted on a custom inflation chamber such that the posterior surface 97 of the LC was aligned with the objective and imaging plane of a Zeiss 710 laser-scanning microscope (LSM 710 NLO, Zeiss, Inc., Oberkochen, Germany) as described previously in Midgett et al. ?. Ocular pressure 99 was set by a water column to a baseline pressure of 5 mmHg and the specimen was allowed to equilibrate 100 for at least 25 minutes prior to imaging to minimize the effects of tissue creep. Duplicate 2×2 tiled z-stacks 101 were acquired back-to-back, with scans starting 300 μ m below the posterior surface and taken at 5 μ m 102 intervals up to the cut surface of the LC, using a Chameleon Ultra II laser tuned to 780 nm. A 390 - 410 nm 103 band pass filter was used to collect the backscattered SHG signal of the collagen structures of the LC using a 10× 0.45 NA Apochromat objective with zoom factor set at 0.7-0.8x depending on the size of the LC. 105 The tiles were imaged at 512×512 pixels and stitched with 15% overlap, which gave an in-plane resolution 106 of 2.37-2.77 µm/pixel, depending on the zoom factor (Supplemental Table S1). Specimens were aligned 107 such that the X direction in the images corresponded to the nasal-temporal direction, Y corresponded to the inferior-superior direction, and Z corresponded to the anterior-posterior direction. Imaging was repeated at the additional pressures of 10 and 45 mmHg.

The SHG image volumes were processed by an iterative deconvolution algorithm (Huygens Essentials, SVI, Hilversum, NL) to reduce noise and blur, and contrast was enhanced with contrast-limited piecewise adaptive histogram equalization (CLAHE) ? in FIJI ?. The shape and area of the LC opening was estimated by importing the z-stack at 5 mmHg for each eye into FIJI and calculating the maximum intensity projection of the SHG volume. The boundary between the LC and oversaturated peripapillary sclera region was defined by picking points manually on the maximum intensity projection. An ellipse was fit to the points using the Matlab function $fit_ellipse$ (Ohad Gal, 2003) and used to segment the LC and sclera. The LC area was estimated as $A = \pi ab$, where a and b were the calculated major and minor axes of the ellipse.

119 2.4 Displacement and strain calculations

125

The Fast-Fourier Iterative DVC (FIDVC) algorithm ? was applied to the enhanced SHG volumes to calculate the 3D displacement of the imaged collagen structures within the LC between 5-10 mmHg and 10-45 mmHg every $4 \times 4 \times 2$ pixels in X, Y, and Z?. This corresponds to a displacement calculation every 8-10 μ m in X and Y and every 10 μ m in Z. The displacement fields between 5-10 and 10-45 mmHg were used to obtain the cumulative displacement between 5-45 mmHg?.

The displacement components, U_X , U_Y , and U_Z were smoothed locally using a Gaussian filter and fit to polynomials in the X,Y,Z directions as shown in Midgett et al. ?. The components of the 3D Green-Lagrange strain tensor in the X-Y plane were evaluated from the gradients of the fit displacement fields U_X, U_Y, U_Z at each grid point X,Y,Z in the posterior LC volume as,

$$E_{XX} = \frac{\partial U_X}{\partial X} + \frac{1}{2} \left(\left(\frac{\partial U_X}{\partial X} \right)^2 + \left(\frac{\partial U_Y}{\partial X} \right)^2 + \left(\frac{\partial U_Z}{\partial X} \right)^2 \right) \tag{1}$$

$$E_{YY} = \frac{\partial U_Y}{\partial Y} + \frac{1}{2} \left(\left(\frac{\partial U_X}{\partial Y} \right)^2 + \left(\frac{\partial U_Y}{\partial Y} \right)^2 + \left(\frac{\partial U_Z}{\partial Y} \right)^2 \right) \tag{2}$$

$$E_{XY} = \frac{1}{2} \left(\frac{\partial U_X}{\partial Y} + \frac{\partial U_Y}{\partial X} + \frac{\partial U_X}{\partial X} \frac{\partial U_X}{\partial Y} + \frac{\partial U_Y}{\partial X} \frac{\partial U_Y}{\partial Y} + \frac{\partial U_Z}{\partial X} \frac{\partial U_Z}{\partial Y} \right). \tag{3}$$

The normal strain components E_{XX} and E_{YY} describe the tensile (positive) or compressive (negative)

strain in the nasal-temporal direction and inferior-superior direction respectively, while the shear strain E_{XY} describes the angle distortion between the X and Y directions. We also calculated the out-of-plane strain components, i.e, E_{ZZ} , E_{XZ} , E_{YZ} ; however, displacements and strains in the Z direction exhibited larger DVC errors and are not reported here (Supplemental Sec. S1.2).

130

131

132

133

136

This analysis differs from a 2D-DIC approach by taking into account the full 3D displacement field in calculating the in-plane Lagrangian strains (Eq. 1-3). The posterior displacement component U_Z describes the posterior bulging of the LC caused by a pressure increase. Including the gradient of U_Z in the strain calculation is needed to account for the contribution of the bulging deformation on the in-plane strains.

The strain components were used to calculate the maximum principal strain E_{max} and the maximum shear strain Γ_{max} in the X-Y plane, which denote the tensile strain and shear strain, respectively, along the directions in which they are maximum:

$$E_{max} = \frac{E_{XX} + E_{YY}}{2} + \sqrt{(\frac{E_{XX} - E_{YY}}{2})^2 + E_{XY}^2}$$
 (4)

$$\Gamma_{max} = \sqrt{(\frac{E_{XX} - E_{YY}}{2})^2 + E_{XY}^2}$$
 (5)

A coordinate transformation was applied to calculate the strain components in cylindrical coordinates, which is more consistent with the cylindrical symmetry of the LC about the central retinal artery and vein (CRAV). The orientation angle θ for a given point in the LC was calculated as the angle between a line connecting the point and the CRAV center, which was manually selected? This orientation angle was used to transform the strain components as follows:

$$E_{rr} = E_{XX}\cos^2\theta + 2E_{XY}\cos\theta\sin\theta + E_{YY}\sin^2\theta \tag{6}$$

$$E_{\theta\theta} = E_{XX} \sin^2 \theta - 2E_{XY} \cos \theta \sin \theta + E_{YY} \cos^2 \theta \tag{7}$$

$$E_{r\theta} = (E_{YY} - E_{XX})\cos\theta\sin\theta - E_{XY}(\sin^2\theta - \cos^2\theta), \tag{8}$$

where E_{rr} and $E_{\theta\theta}$ denote the radial and circumferential strain of the LC. The posterior bowing and in-plane expansion of the LC both contribute to E_{rr} , while $E_{\theta\theta}$ arises only from the radial expansion of the LC.

The baseline positional errors and the DVC displacement and strain errors were estimated for each

specimen (Supplemental Sec. S1) as shown previously ?. The baseline positional error, which includes 137 factors such as creep, was estimated for all specimens by correlating the 2 duplicate image sets acquired at 138 5 mmHg with DVC and summarized as the average and average magnitude of the displacements U_X, U_Y, U_Z 139 (Supplemental Table S1). DVC correlation errors were estimated by applying a numerical displacement and stretch to one of the duplicate image volumes at 5 mmHg and correlating it with DVC to the second, 141 undeformed image volume. DVC errors were summarized as the average and average absolute difference 142 between the DVC calculations and the numerically applied displacements and strains (Supplemental Table S2-S3). DVC displacement error fields and the DVC correlation coefficient were used to mask regions 144 within the image volume that were dark or had X and Y displacement errors greater than 2 μ m as previously 145 described?. Displacement and strain errors in the LC were averaged through all 26 eyes to obtain an estimate 146 of the average DVC resolution within a typical LC. The average displacement error was less than $0.8 \mu m$ 147 for U_X , 0.6 μ m for U_Y , and 3.6 μ m for U_Z . Average strain errors were less than 0.28% for E_{XX} , 0.25% for 148 E_{YY} , and 0.16% for E_{XY} .

2.5 Statistical analysis

The LC was divided into 8 anatomical regions as described previously ?. The center of the central retinal artery and vein (CRAV) was picked manually on the maximum intensity projection of the SHG image and a cylindrical region of radius 200 μ m was defined surrounding the CRAV. The central (1) and peripheral (2) LC regions were divided at the midpoint distance between the LC boundary and the boundary of the CRAV region. The central and peripheral regions were further divided into the superior (S), inferior (I), temporal (T), and nasal (N) quadrants using 45° and 135° bisectors as shown in Figure ??.

The strain measures E_{XX} , E_{YY} , E_{rr} , $E_{\theta\theta}$, E_{max} , and Γ_{max} between 5-10 and 5-45 mmHg were averaged over the LC in each eye and in the 8 regions of the LC. General linear models were used to test for: 1) associations between age and LC strain; 2) differences in eye length, LC area, and average LC strains between glaucoma and normal eyes; 3) differences in average LC strains between eye pairs from the same donor with the same or different levels of axonal loss; 4) differences in average LC strain between the undamaged normal group (NU, n = 8), the more mildly damaged glaucoma group (GM, n = 9), and more severely damaged glaucoma group (GS, n = 6); 5) differences between central and peripheral LC strains in

the NU, GM, and GS groups; and 6) differences between the central nasal, temporal, superior, and inferior 164 quadrant strains in the NU, GM and GS groups. When comparing between glaucoma and normal eyes 165 and between NU, GM, and GS groups, the analysis was performed for both including and excluding the 166 uncertain glaucoma eyes listed in Table ??. In Eye 12, the 2×2 tiled z-stacks acquired at 45 mmHg failed to 167 stitch together, so this eye was excluded in the analysis of strains between 5-45 mmHg. In eye 26, the optic 168 nerve damage was ungradable so this eye was excluded from comparisons grouping eyes by level of axonal 169 damage (NU, GM, GS). Eye length measurements were not taken for the first 3 eyes tested (1-3) so these 170 eyes are excluded from comparisons of eye length. The peripheral LC quadrants were not compared because 171 eyes with glaucoma damage often had poor peripheral correlation with one or more missing quadrants. 172

For analyses with one measurement per eye, such as the specimen-averaged strain outcomes, LC area, 173 and eye length, all estimates and p-values are from general linear models, which take into account correlations 174 between the 2 eyes of a single donor. For all outcomes, the normal distribution function and the link identity 175 function were used with the linear models. For analysis of data with more than one measurement per eye, 176 all estimates and p-values are from linear mixed models which take into account the clustering of the 2 eyes for a donor as well as correlations among the measurements from a single eye. Measurements from different 178 LC regions were assumed to have a compound symmetry correlation structure, in which the measurements 179 from any 2 regions have the same correlation. In the text, means and standard deviations are both estimated from the raw data. All p-values are from regression models and least squares means from the models were 181 used to estimate mean outcomes and 95% confidence intervals. The Bonferroni method was used to adjust 182 significance levels for multiple pairwise comparisons of a dependent variable, such as in the analysis for the 183 differences in the strain outcomes between the 3 categories of axon loss and the 4 quadrants. A comparison 184 was considered significant if the p-value (or adjusted p-value, where applicable) was less than or equal to 185 0.05. All analyses were performed using SAS 9.2 (SAS Institute, Cary, NC). 186

87 **Results**

188 3.1 LC geometry

Eye length in the normal group $(23.7\pm0.3 \text{ mm}, n=7)$ was significantly smaller (p=0.005, Table ??, Fig.)

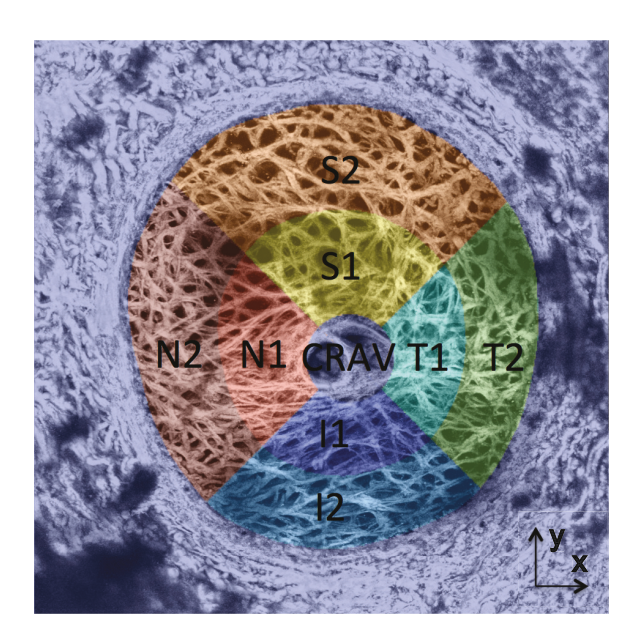


Figure 1: Illustration of the segmentation of the LC from the PPS and the 8 LC regions studied.

??a) than eye length in the glaucoma group $(24.5\pm0.8 \text{ mm}, n = 16)$. LC area in the normal group $(3.37\pm0.51 \text{ mm}^2, n = 10)$ was also significantly smaller (p = 0.03, Table ??, Fig. ??b) than LC area of the glaucoma group $(3.80\pm0.37 \text{ mm}^2, n = 16)$. Eye length and LC area did not vary significantly between the GM and GS groups and was larger in both groups on average compared to normals (Table ??).

Excluding the 3 uncertain glaucoma eyes in Table ?? from the analyses changed the p-values, but did not substantively alter the findings. The LC area (p = 0.03) and eye length (p = 0.02) remained smaller in the normal compared to glaucoma group. The LC area (p = 0.002) and eye length (p = 0.03) also differed between the different groups of axon loss. In *post-hoc* pair-wise tests, the LC area was larger for the GM than NU group (adjusted p = 0.01) and larger in the GM than GS group (adjusted p = 0.004). The axial length was larger for the GS than NU group (adjusted p = 0.03)

200 3.2 Strain outcomes

194

195

196

197

198

199

Contours of the strains E_{rr} , $E_{\theta\theta}$, and E_{max} are plotted in the LC for eye 6 (NU), eye 17 (GM), and eye 14 (GS) in Figure 3 and for all specimens in Supplemental Figures S2-S27. Compared across all specimens at 45 mmHg (n=25), maximum principal strain E_{max} (2.30% \pm 0.78%) was the largest of the LC strain outcomes. The normal strain components were of similar average magnitude ($E_{XX}=1.02\%\pm0.42\%$, $E_{YY}=1.02\%\pm0.42\%$) outcomes.

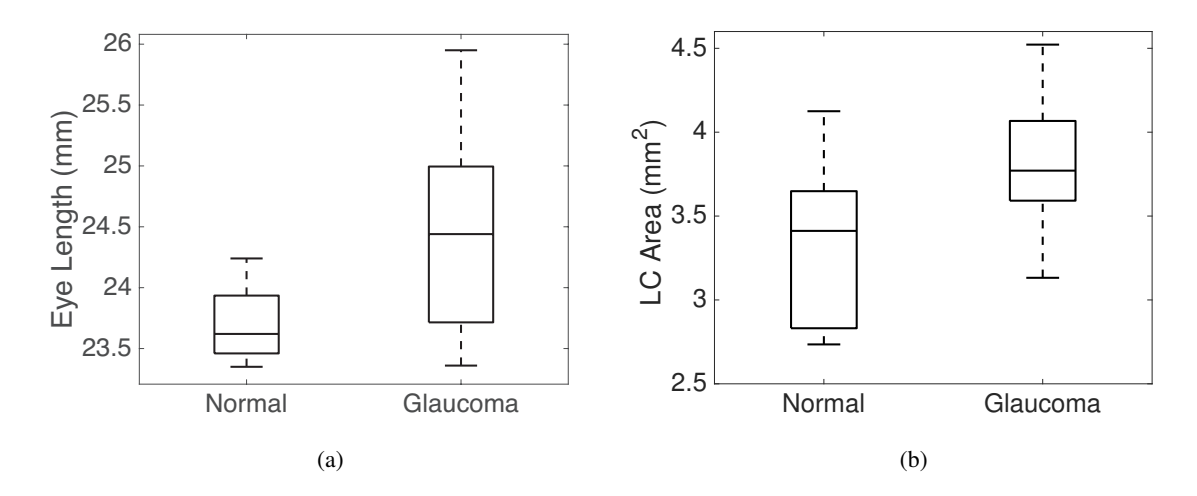


Figure 2: Comparison of a) eye length (p = 0.005) and b) LC area (p = 0.03) in eyes diagnosed with glaucoma (n = 16) and normals.

Outcome Group		Number	Estimated Mean	p-value
		of Eyes	Outcome (95% CI)	
Eye Length (mm)	Glaucoma	16	24.47 (23.98, 24.96)	0.005
	Normal	7*	23.74 (23.59, 23.88)	
LC Area (mm ²)	Glaucoma	16	3.81 (3.60, 4.02)	0.03
	Normal	10	3.35 (2.98, 3.72)	

Table 3: Comparison of eye length and LC area between normal (n = 10) and glaucoma (n = 16) groups. Eye length and LC area were significantly larger $(p \le 0.03)$ in eyes diagnosed with glaucoma compared to normals. * eye length was not measured for the first 3 eyes tested (n = 7) for eye length and n = 10 for LC area).

Outcome	Group	Number	Estimated Mean	Pairwise	p-value	Adjusted*
		of Eyes	Outcome (95% CI)	Comparison		p-value
Eye Length (mm)	GS	6	24.42 (24.01, 24.83)	GS - GM	0.80	1.00
	GM	9	24.45 (23.89, 25.01)	GS - NU	0.002	0.01
	NU	6	23.72 (23.54, 23.90)	GM - NU	0.01	0.04
LC Area (mm ²)	GS	6	3.64 (3.40, 3.88)	GS - GM	0.22	0.65
	GM	9	3.90 (3.58, 4.21)	GS - NU	0.12	0.37
	NU	8	3.28 (2.89, 3.67)	GM - NU	0.02	0.05

Table 4: Comparison of eye length and LC area between NU (n = 8), GM (n = 9), and GS (n = 6) groups. Eye length was significantly larger $(p \le 0.04)$ in both GS and GM groups compared to the NU group and similar between the GM and GS groups. LC area was significantly larger (p = 0.05) in the GM group compared to the NU group, but there was no significant difference in LC area between the GS and NU groups or the GM and GS groups. * p-value adjusted for multiple comparisons.

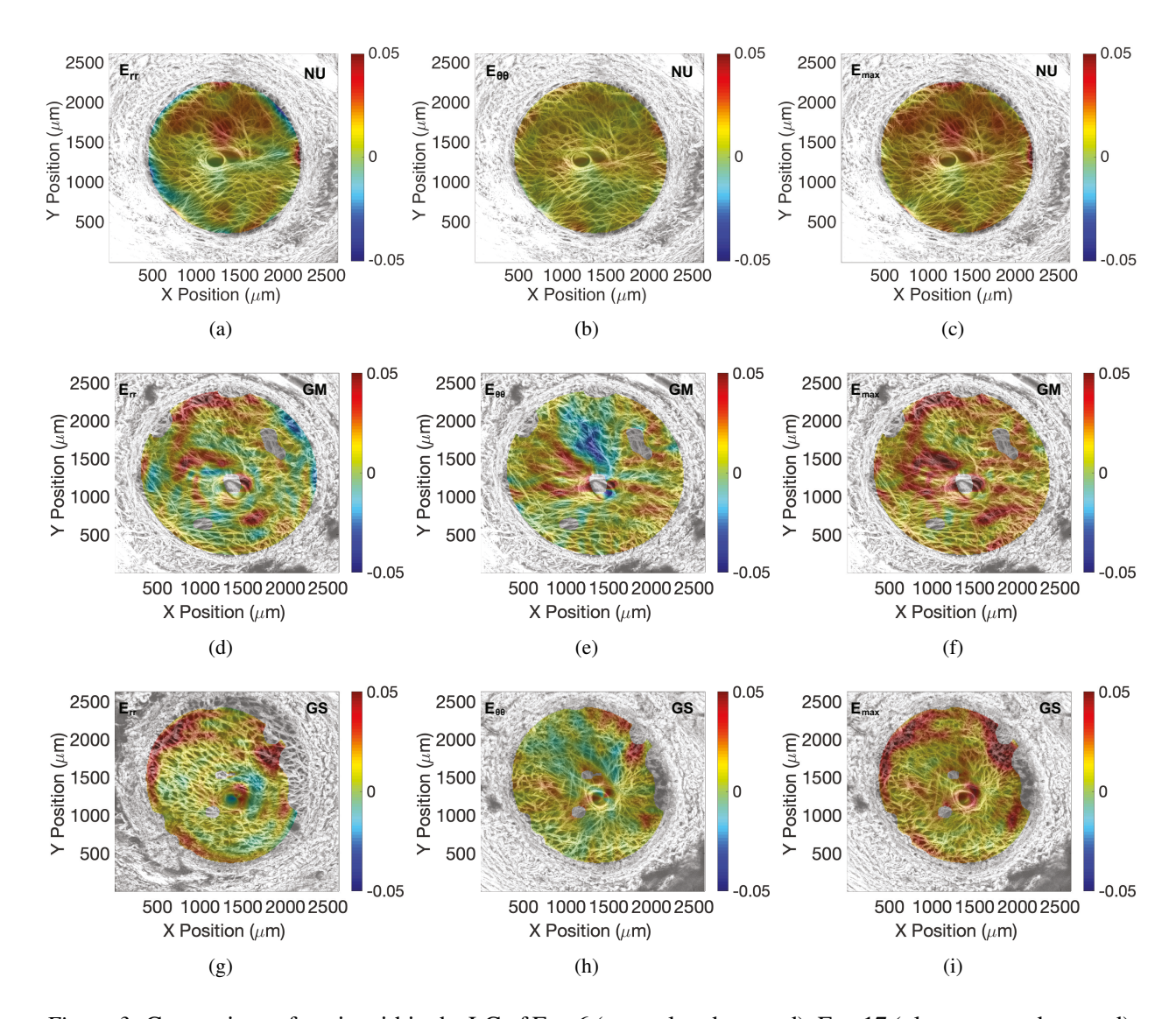


Figure 3: Comparison of strain within the LC of Eye 6 (normal undamaged), Eye 17 (glaucoma undamaged), and Eye 14 (glaucoma severely-damaged) for an inflation of 5 to 45 mmHg. Eye 2: a) E_{rr} , b) $E_{\theta\theta}$, c) E_{max} ; Eye 17: d) E_{rr} , e) $E_{\theta\theta}$, f) E_{max} ; and Eye 14: g) E_{rr} , h) $E_{\theta\theta}$, i) E_{max} . Holes in the strain color contours were regions that either had poor correlation coefficients or high displacement error estimates. These were removed from the strain calculations.

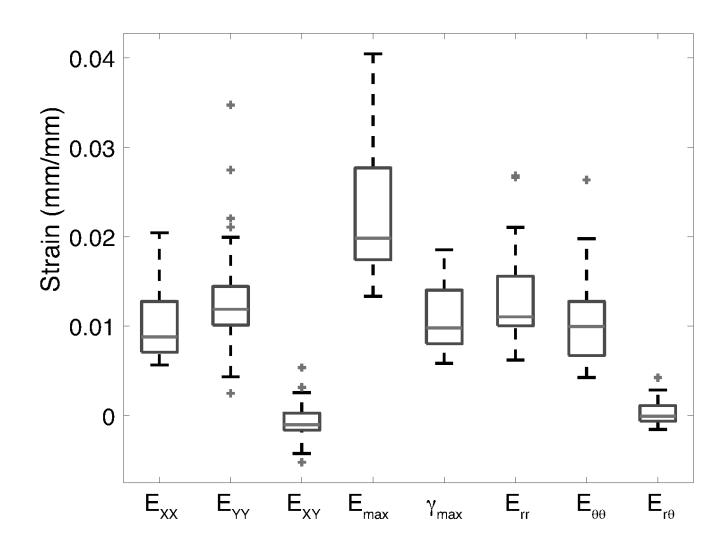


Figure 4: Comparison of strain outcomes of all specimens for inflation from 5-45 mmHg (n = 25).

Strain Outcomes	Number of	Estimated Strain	p-value
45 mmHg	Measures	(95% CI)	
E_{XX}	25	0.0102 (0.0085, 0.0120)	< 0.0001
E_{YY}	25	0.0138 (0.0108, 0.0167)	< 0.0001
E_{XY}	25	-0.0006 (-0.0015, 0.0003)	0.21
E_{max}	25	0.0230 (0.0200, 0.0260)	< 0.0001
Γ_{max}	25	0.0110 (0.0096, 0.0125)	< 0.0001
E_{rr}	25	0.0133 (0.0107, 0.0158)	< 0.0001
$E_{m{ heta}m{ heta}}$	25	0.0108 (0.0086, 0.0130)	< 0.0001
$E_{r heta}$	25	0.0003 (-0.0003, 0.0010)	0.32

Table 5: Linear models were used to estimate the significance of average strain in all eyes at 45 mmHg (n=25). Normal strain components were positive and significantly greater than zero (p < 0.0001), but shear strain components were near-zero on average (p > 0.3).

1.37% \pm 0.70, $E_{rr} = 1.32\% \pm 0.57\%$, $E_{\theta\theta} = 1.07\% \pm 0.55\%$) and were positive and significantly greater than zero (p < 0.0001, Table ??), showing that LC deformation from pressure increase was on average equibiaxial tension in the plane of the tissue (LC expansion). The average shear strains $E_{XY} = -0.06\% \pm 0.23\%$ and $E_{r\theta} = 0.03\% \pm 0.14\%$ were near-zero on average (p > 0.2, Table ??), but maximum shear strain was significant $\Gamma_{max} = 1.1\% \pm 0.39\%$ (p < 0.0001, Table ??) because of local regions of large positive and negative shear strains.

Strain Outcomes	Number of	Estimated strain change	p-value
45 mmHg	Measures	per 1 year in age (95% CI)	
E_{XX}	25	-0.000054 (-0.000379, 0.000271)	0.74
E_{YY}	25	0.000376 (-0.000049, 0.000800)	0.08
E_{max}	25	0.000223 (-0.000241, 0.000686)	0.35
Γ_{max}	25	0.000061 (-0.000177, 0.000298)	0.62
E_{rr}	25	0.000167 (-0.000235, 0.000568)	0.42
$E_{ heta heta}$	25	0.000156 (-0.000207, 0.000520)	0.40

Table 6: Linear models were used to investigate the variation of strain with age in all eyes at 45 mmHg (n = 25). Strain measures did not vary significantly with age $(p \ge 0.08)$.

211 3.2.1 Effects of Age

Average LC strains did not vary significantly with age between 5-10 or 5-45 mmHg for the narrow and older age range (76-90+) of this study ($p \ge 0.08$, Table ??, Supplemental Table S6-S7).

214 3.2.2 Effect of glaucoma diagnosis

The normal strain components and the maximum principal strain were generally smaller for diagnosed 215 glaucoma eyes than for normal eyes at 10 and 45 mmHg (Tabs. ??-??). At 10 mmHg, E_{XX} was 38% smaller 216 (p=0.02), $E_{\theta\theta}$ was 46% smaller (p=0.05), E_{max} was 32% smaller (p=0.08), and E_{rr} was 36% smaller 217 (p = 0.08) in glaucoma eyes (n = 16) compared to normals (n = 10) (Table ??). At 45 mmHg, $E_{\theta\theta}$ was 35% 218 smaller (p = 0.03) and E_{XX} was 25% smaller (p = 0.07) in glaucoma eyes (n = 15) compared to normals 219 (n = 10) (Table ??). 220 Excluding the 3 uncertain glaucoma eyes in Table ?? caused the difference in the normal strains at 10 221 mmHg between normal and diagnosed glaucoma eyes to become less significant for E_{XX} (p = 0.03) but 222 more significant for $E_{\theta\theta}$ (p=0.03), and E_{max} (p=0.06), and unchanged for E_{rr} . Moreover, the difference 223 in E_{YY} became nearly significant p=0.08. Similarly at 45 mmHg, the difference in $E_{\theta\theta}$ became more 224

significant (p = 0.02), but the difference in E_{XX} became nonsignificant (p = 0.15).

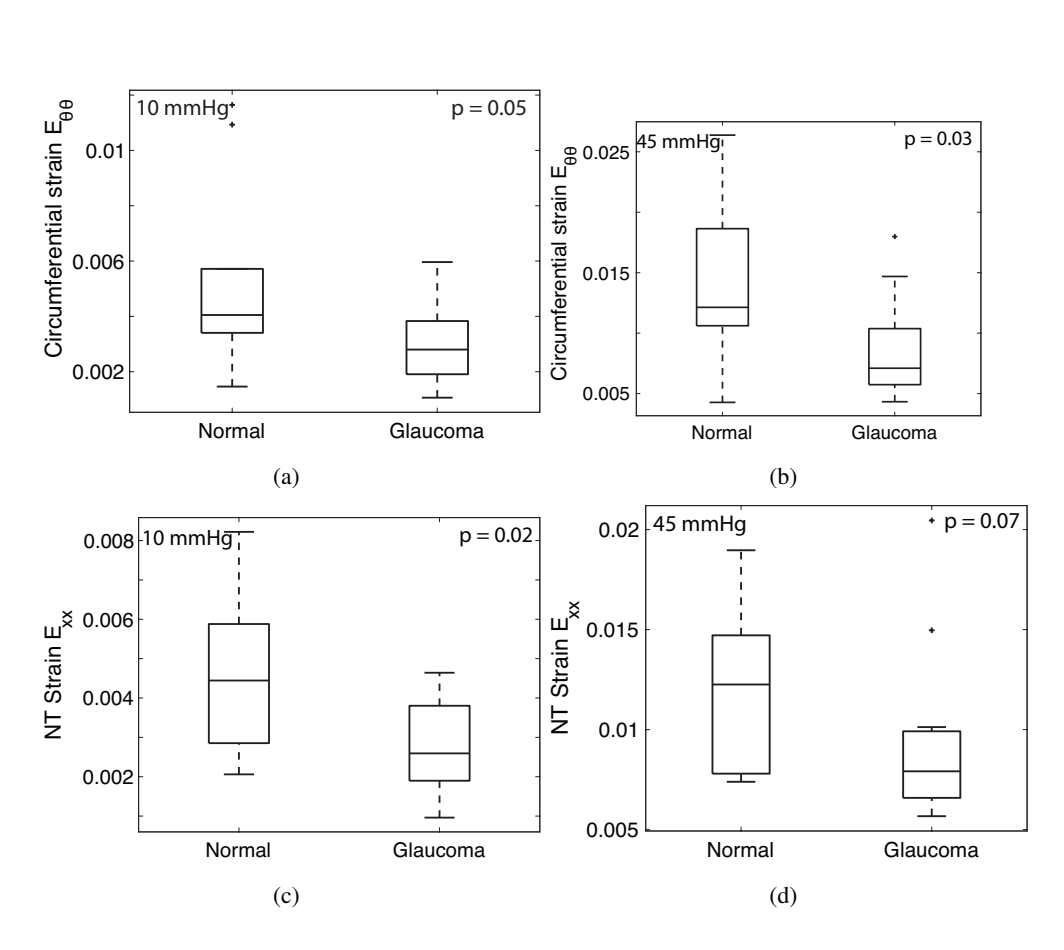


Figure 5: Comparison of average LC strain in normal and glaucoma eyes showing a) $E_{\theta\theta}$ at 10 mmHg, b) $E_{\theta\theta}$ at 45 mmHg, c) E_{XX} at 10 mmHg, and d) E_{XX} at 45 mmHg.

Strain Outcomes	Group	Number	Estimated Mean	p-value
10 mmHg		of Eyes	Outcome (95% CI)	
E_{XX}	Glaucoma	16	0.0028 (0.0022, 0.0033)	0.02
	Normal	10	0.0045 (0.0032, 0.0059)	
E_{YY}	Glaucoma	16	0.0038 (0.0030, 0.0047)	0.12
	Normal	10	0.0067 (0.0031, 0.0103)	
E_{max}	Glaucoma	16	0.0071 (0.0060, 0.0082)	0.08
	Normal	10	0.0105 (0.0069, 0.0140)	
Γ_{max}	Glaucoma	16	0.0038 (0.0032, 0.0043)	0.20
	Normal	10	0.0048 (0.0033, 0.0064)	
E_{rr}	Glaucoma	16	0.0037 (0.0031, 0.0043)	0.08
	Normal	10	0.0058 (0.0036, 0.0080)	
$E_{\theta\theta}$	Glaucoma	16	0.0029 (0.0022, 0.0036)	0.05
	Normal	10	0.0054 (0.0030, 0.0078)	

Table 7: Comparison of LC strain at 10 mmHg between normal (n = 10) and glaucoma (n = 16) groups. E_{XX} and $E_{\theta\theta}$ were significantly smaller $(p \le 0.05)$ and E_{max} and E_{rr} were borderline significantly smaller (p = 0.08) in glaucomas compared to normals.

Strain Outcomes	Group	Number	Estimated Mean	p-value
45 mmHg		of Eyes	Outcome (95% CI)	
$\overline{E_{XX}}$	Glaucoma	15	0.0090 (0.0070, 0.0110)	0.07
	Normal	10	0.0120 (0.0095, 0.0146)	
$\overline{E_{YY}}$	Glaucoma	15	0.0119 (0.0100, 0.0137)	0.16
	Normal	10	0.0166 (0.0103, 0.0230)	
E_{max}	Glaucoma	15	0.0211 (0.0182, 0.0240)	0.13
	Normal	10	0.0258 (0.0204, 0.0313)	
Γ_{max}	Glaucoma	15	0.0106 (0.0091, 0.0122)	0.52
	Normal	10	0.0116 (0.0089, 0.0144)	
$\overline{E_{rr}}$	Glaucoma	15	0.0121 (0.0097, 0.0144)	0.30
	Normal	10	0.0149 (0.0102, 0.0197)	
$E_{\theta\theta}$	Glaucoma	15	0.0088 (0.0071, 0.0106)	0.03
	Normal	10	0.0136 (0.0096, 0.0176)	

Table 8: Comparison of LC strain at 45 mmHg between normal (n = 10) and glaucoma (n = 15) groups. $E_{\theta\theta}$ was significantly smaller (p = 0.03) and E_{XX} was borderline significantly smaller (p = 0.07) in glaucomas compared to normals.

226 3.2.3 Effect of optic nerve damage

We next compared the LC strains for the eyes separated into 3 groups depending on their glaucoma diagnosis 227 and level of axon loss: undamaged normals (NU, n = 8), more mildly damaged glaucomas (GM, n = 9 for 228 10 mmHg and n = 8 for 45 mmHg), and more severely damaged glaucomas (GS, n = 6). For the normal 229 (tensile) strain components and the maximum principal strain, the average for the GM and GS groups tended 230 to be lower than the NU group. However, only E_{XX} differed significantly between the different optic nerve 231 damage groups (p = 0.003) at 45 mmHg (Table ??). In a post-hoc pairwise comparison, E_{XX} was 40% 232 smaller in the GM group compared to the NU group (adjusted p = 0.01) and 33% smaller than in the GS 233 group, though the latter was not significant (adjusted p = 0.11, Fig. ??b). Though comparisons were not 234 significant for the other strain outcomes, nearly all of the strain outcomes were smaller in the GM group 235 than the NU group (Supplemental Table S8-S9). At 45 mmHg, all of the normal strain components in the GM group were also smaller than in the GS group (Supplemental Table S9). 237

Excluding the 3 uncertain glaucoma eyes reduced the number of eyes in the GM group to n = 6 at 238 10 mmHg and n = 5 at 45 mmHg, but it generally increased the significance of the comparisons (Table 239 ??). At 10 mmHg, both E_{XX} and E_{YY} were significantly different between the 3 groups ($p \le 0.0001$). In 240 post-hoc pairwise comparisons, E_{XX} was significantly larger while E_{YY} was significantly smaller in the more 241 mildly damaged GM than more severely damaged GS glaucoma groups (adjusted $p \le 0.0003$) and E_{XX} was 242 nearly significantly larger in the NU than GS group (adjusted p = 0.07). The p-values for E_{max} and $E_{\theta\theta}$ 243 also decreased to p = 0.17, though they remained above the significance threshold. At 45 mmHg, E_{XX} 244 remained significantly different between the groups, though with a higher p = 0.01, and larger for the NU 245 than GM group (adjusted p=0.03). In addition, the comparisons became significant for $E_{\theta\theta}$ (p = 0.01), where $E_{\theta\theta}$ was significantly larger for the NU than GM group (adjusted p=0.02), and nearly significant for 247 E_{max} (p = 0.09). 248

249 3.2.4 Regional strain variation

The strain outcomes measured at 45 mmHg were averaged within the central and peripheral LC regions for each damage group NU, GM, and GS to compare for differences in radial strain variation. In the NU group (n = 8), Γ_{max} was significantly larger in the peripheral LC compared to central regions (p = 0.02)

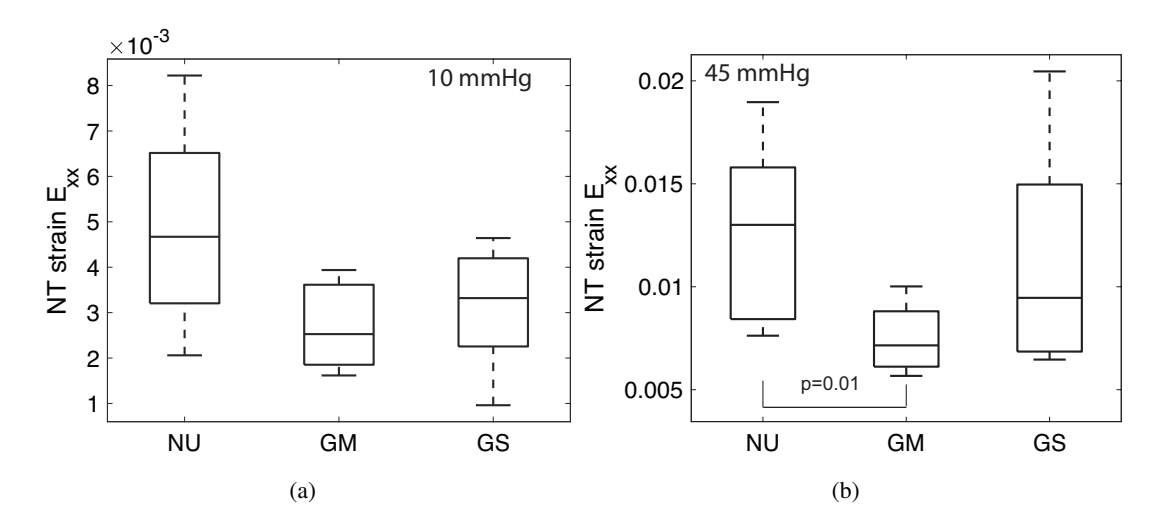


Figure 6: Comparison of E_{XX} strain between undamaged normals (NU), more mildly damaged glaucomas (GM), and more severely damaged glaucomas (GS) at a) 10 mmHg and b) 45 mmHg. The number of specimens were NU: n = 8, GM: n = 9 for 10 mmHg and n = 8 for 45 mmHg), GS: n = 6. The E_{XX} strain in glaucoma eyes was smaller but not significantly less than in normals at 10 mmHg at all axon loss levels, but at 45 mmHg, strain was only significantly smaller in undamaged or mildly-damaged glaucoma eyes.

Strain Outcome	Group	Number	Estimated Mean	p-value	Pairwise	p-value	Adjusted*
		of Eyes	Outcome (95% CI)		Comparison		p-value
E_{XX}	GS	6	0.0028 (0.0018, 0.0038)		GS - GM	0.63	1.00
10 mmHg	GM	9	0.0030 (0.0023, 0.0036)	0.11	GS - NU	0.04	0.11
	NU	8	0.0047 (0.0032, 0.0063)		GM - NU	0.04	0.13
E_{XX}	GS	6	0.0113 (0.0080, 0.0146)		GS - GM	0.04	0.11
45 mmHg	GM	8	0.0075 (0.0064, 0.0085)	0.003	GS - NU	0.58	1.00
	NU	8	0.0126 (0.0094, 0.0159)		GM - NU	0.003	0.01

Table 9: Comparison of E_{XX} at 10 and 45 mmHg between the normal undamaged (NU), glaucoma undamaged and mildly-damaged (GM) and glaucoma moderately- and severely-damaged (GS) groups. Comparisons that were statistically significant are in bold.

Strain Outcome	Group	Number	Estimated Mean	p-value	Pairwise	p-value	Adjusted*
		of Eyes	Outcome (95% CI)		Comparison		p-value
E_{XX}	GS	6	0.0026 (0.0016, 0.0036)		GS - GM	<0.0001	<0.0003
10 mmHg	GM	6	0.0035 (0.0025, 0.0045)	< 0.0001	GS - NU	0.02	0.07
	NU	8	0.0047 (0.0032, 0.0062)		GM - NU	0.18	0.55
E_{XX}	GS	6	0.0113 (0.0080, 0.0146)		GS - GM	0.07	0.21
45 mmHg	GM	5	0.0079 (0.0066, 0.0092)	0.01	GS - NU	0.57	1.00
	NU	8	0.0126 (0.0094, 0.0159)		GM - NU	0.01	0.03
$\overline{E_{YY}}$	GS	6	0.0040 (0.0027, 0.0052)		GS - GM	<0.0001	<0.0003
10 mmHg	GM	6	0.0034 (0.0020, 0.0047)	0.0001	GS - NU	0.37	1.00
	NU	8	0.0055 (0.0025, 0.0085)		GM - NU	0.21	0.62
E_{YY}	GS	6	0.0124 (0.0079, 0.0169)		GS - GM	0.58	1.00
45 mmHg	GM	5	0.0112 (0.0093, 0.0130)	0.44	GS - NU	0.55	1.00
	NU	8	0.0146 (0.0092, 0.0199)		GM - NU	0.24	0.71
$E_{\theta\theta}$	GS	6	0.0029 (0.0016, 0.0041)		GS - GM	0.66	1.00
10 mmHg	GM	6	0.0026 (0.0019, 0.0034)	0.17	GS - NU	0.13	0.38
	NU	8	0.0048 (0.0026, 0.0069)		GM - NU	0.06	0.19
$E_{\theta\theta}$	GS	6	0.0097 (0.0063, 0.0132)		GS - GM	0.12	0.37
45 mmHg	GM	5	0.0067 (0.0052, 0.0082)	0.01	GS - NU	0.34	1.00
	NU	8	0.0122 (0.0086, 0.0158)		GM - NU	0.01	0.02

Table 10: Comparison of E_{XX} E_{YY} and $E_{\theta\theta}$ at 10 and 45 mmHg between the normal undamaged (NU), more mildly damaged glaucoma (GM) and more severely damaged glaucoma (GS) groups, excluding the 3 uncertain glaucoma eyes. The strains generally were smaller in the GM and GS groups compared to the NU group. Comparisons that were statistically significant are in bold.

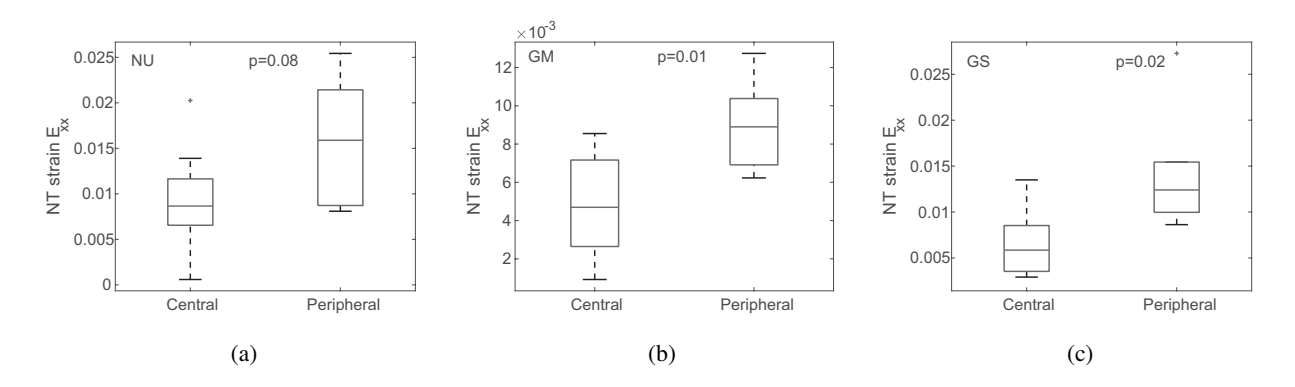


Figure 7: Comparison of E_{XX} at 45 mmHg in the central and peripheral LC for the a) NU, b) GM, and c) GS groups.

and E_{XX} was borderline significantly larger in the peripheral LC region (p = 0.08) (Table ??). In the GM group (n = 8), only E_{XX} was significantly larger in the peripheral LC region compared to the central region (p = 0.01, Table ??). In the GS group (n = 6), all of the normal strain components, E_{XX} , E_{YY} , E_{max} , E_{rr} , and $E_{\theta\theta}$, were all significantly larger in the peripheral LC region compared to the central LC region ($p \leq 0.05$) and Γ_{max} was borderline significantly larger in the peripheral LC region (p = 0.08) (Table ??).

The results suggested that the LC strain response for more severely damaged glaucoma eyes (GS) had the largest difference between central and peripheral. To test this hypothesis, we compared the ratio of the averaged peripheral to central maximum principal strain E_{max} and maximum shear strain γ_{max} between the three groups. The ratio of E_{max} in the peripheral LC to central LC for inflation from 5-10 mmHg was significantly different between the 3 groups (p = 0.01). The ratio was similar between the GM and NU (1.28 and 1.33), but was 20% larger in the GS (1.47) than GM group (adjusted p = 0.004). The ratio of peripheral to central LC strains were also larger in the GS than GM groups at 45 mmHg, but the analysis was not statistically significant. The results did not substantively change when we excluded the 3 uncertain glaucoma eyes from the analysis. The difference in the ratio of E_{max} in the peripheral to central LC at 10 mmHg became more significant (p = 0.0001) as did the difference between GS and GM (adjusted p = 0.0003) in the *post-hoc* pairwise comparisons.

NU Group	LC Location	Number of	Estimated Mean	p-value
Strain, 45 mmHg		Measures	Outcome (95% CI)	
E_{XX}	Central	8	0.0094 (0.0040, 0.0147)	0.08
	Peripheral	8	0.0157 (0.0104, 0.0211)	
E_{YY}	Central	8	0.0152 (0.0080, 0.0224)	0.93
	Peripheral	8	0.0150 (0.0077, 0.0222)	
E_{max}	Central	8	0.0214 (0.0127, 0.0301)	0.10
	Peripheral	8	0.0290 (0.0202, 0.0377)	
Γ_{max}	Central	8	0.0091 (0.0042, 0.0139)	0.02
	Peripheral	8	0.0136 (0.0087, 0.0184)	
E_{rr}	Central	8	0.0120 (0.0043, 0.0197)	0.28
	Peripheral	8	0.0174 (0.0098, 0.0251)	
$E_{\theta\theta}$	Central	8	0.0125 (0.0072, 0.0177)	0.70
	Peripheral	8	0.0131 (0.0079, 0.0184)	

Table 11: Comparison of LC strain in central and peripheral LC regions of undamaged normal (NU) eyes (n = 8). Γ_{max} was significantly higher in the peripheral LC region compared to the central region (p = 0.02). E_{XX} was borderline significantly higher in the peripheral LC region compared to the central region $(p \le 0.08)$.

GM Group	LC Location	Number of	Estimated Mean	p-value
Strain, 45 mmHg		Measures	Outcome (95% CI)	
E_{XX}	Central	8	0.0048 (0.0028, 0.0068)	0.01
	Peripheral	8	0.0089 (0.0069, 0.0109)	
E_{YY}	Central	8	0.0111 (0.0073, 0.0149)	0.76
	Peripheral	8	0.0118 (0.0080, 0.0157)	
E_{max}	Central	8	0.0178 (0.0126, 0.0230)	0.37
	Peripheral	8	0.0211 (0.0159, 0.0263)	
Γ_{max}	Central	8	0.0097 (0.0062, 0.0133)	0.67
	Peripheral	8	0.0106 (0.0071, 0.0142)	
E_{rr}	Central	8	0.0083 (0.0051, 0.0115)	0.12
	Peripheral	8	0.0121 (0.0089, 0.0153)	
$E_{\theta\theta}$	Central	8	0.0077 (0.0042, 0.0111)	0.38
	Peripheral	8	0.0088 (0.0053, 0.0123)	

Table 12: Comparison of LC strain in central and peripheral LC regions of more mildly damaged glaucoma (GM) eyes (n = 8). E_{XX} was significantly higher in the peripheral LC region compared to the central region (p = 0.01).

GS Group	LC Location	Number of	Estimated Mean	p-value
Strain, 45 mmHg		Measures	Outcome (95% CI)	
E_{XX}	Central	6	0.0067 (0.0012, 0.0122)	0.02
	Peripheral	6	0.0144 (0.0088, 0.0199)	
E_{YY}	Central	6	0.0088 (0.0013, 0.0163)	0.03
	Peripheral	6	0.0154 (0.0079, 0.0229)	
E_{max}	Central	6	0.0154 (0.0051, 0.0256)	0.03
	Peripheral	6	0.0273 (0.0170, 0.0376)	
Γ_{max}	Central	6	0.0076 (0.0032, 0.0119)	0.08
	Peripheral	6	0.0124 (0.0081, 0.0168)	
E_{rr}	Central	6	0.0079 (0.0004, 0.0154)	0.01
	Peripheral	6	0.0191 (0.0116, 0.0266)	
$E_{\theta\theta}$	Central	6	0.0077 (0.0023, 0.0130)	0.02
	Peripheral	6	0.0106 (0.0053, 0.0160)	

Table 13: Comparison of LC strain in central and peripheral LC regions of more severly damaged glaucoma (GS) eyes (n = 6). E_{XX} , E_{YY} , E_{max} , E_{rr} , and $E_{\theta\theta}$ were significantly higher in the peripheral LC region compared to the central region ($p \le 0.03$).

269 4 Discussion

We applied the ex vivo inflation test developed by Midgett et al. ? to measure the strains in the LC 270 of enucleated normal and glaucoma eyes caused by inflation from 5-10 mmHg and 5-45 mmHg. The 271 strain outcomes were compared between normal and diagnosed glaucoma groups and between groups with 272 different axonal damage levels. The specimen-averaged normal strains were smaller in the LC of diagnosed 273 glaucoma eyes than in normal eyes. The comparisons were statistically significant for the nasal-temporal 274 E_{XX} and circumferential $E_{\theta\theta}$ strains for inflation from 5-10 mmHg and for $E_{\theta\theta}$ for inflation from 5-45 mmHg. Excluding the 3 uncertain glaucoma eyes decreased the p-values (making the results more significant) 276 for $E_{\theta\theta}$ and increased the p-values for E_{XX} , but did not otherwise alter the findings. The LC strains also 277 differed between different damage groups. The average normal (tensile) strain components for the mildly 278 damaged glaucoma GM and more severely damaged glaucoma GS groups tended to be smaller than for the 279 undamaged normal NU group. At 45 mmHg, the average normal strains also trended smaller for the GM 280 than GS group. However, the comparison was only statistically significant for E_{XX} at 45 mmHg between 281 the GM and NU groups. When we excluded the 3 uncertain glaucoma eyes, the comparison between the 282 three groups became statistically significantly for more strain components, specifically for E_{XX} and E_{YY} at 283

 284 10 mmHg and E_{XX} and $E_{\theta\theta}$ at 45 mmHg. Smaller strains indicate a stiffer structural response of the LC in glaucoma eyes compared to normal eyes. This is consistent with a number of previous findings for the eye, sclera and ONH tissues, including *in vivo* measurement of a stiffer ocular rigidity in glaucoma patients ?, measurements of a stiffer displacement response of the ONH in human *post-mortem* eyes ?, a stiffer elastic modulus of *post-mortem* monkey sclera with experimental glaucoma ?, a stiffer pressure-strain response of the human peripapillary sclera with glaucoma ???, and smaller anterior lamina displacement by *in vivo* ONH imaging with worse glaucoma damage ?.

A number of factors can affect the strain outcomes measured for the inflation response of the LC, including age, geometry of the eye, LC and sclera, and material properties of the LC and sclera. Previous studies showed a significant stiffening effect with age, where nearly all strain outcomes decreased with age for a broad age range of 26-90+ years ??. However, we did not find a significant correlation between strain and age for the narrower and older age range of 75-90+ used in this study. This indicated that age-related variations did not contribute to the smaller strains measured for the diagnosed glaucoma group than the normal group, nor to the differences in strains between the different axonal damage groups.

The eye length of glaucoma eyes was on average 3% longer than in normal eyes. Based on Laplace's law for a thin spherical shell, a larger eye length would result in higher IOP-induced tensile hoop stresses in the sclera and higher LC strains rather than the smaller LC strains measured here for glaucoma eyes. However, the post-mortem measurements of the lengths of the enucleated eyes were not made at the test pressures, thus differences in eye lengths and their effects on the hoop stresses and measured LC strain response to inflation may have been underestimated or overestimated in this discussion. The average LC area was 14% larger in glaucoma than normal eyes, which is consistent with previous findings that a larger LC area is associated with greater glaucoma prevalence ??. We measured in a prior study of 10 normal human eyes with a similar range of LC area (2.6-4.1 mm²) but a broader age range (26-73 years) that LC strains increased with LC area ?. This was opposite of the finding in this study that glaucoma eyes with larger LC area exhibited smaller strains, indicating that LC strains would be even less in glaucoma eyes compared to normal eyes if the two groups had similar eye lengths and LC areas.

The larger structural stiffness of the LC in glaucoma eyes may be caused in part by glaucoma-related remodeling of the sclera. Previous studies of *post-mortem* human eyes reported a stiffer inflation response

of the sclera ?? and an altered anisotropic collagen fiber structure in the peripapillary sclera of glaucoma eyes ??. Studies in animal models of glaucoma using similar methods have shown that the inflation response 313 of the sclera becomes stiffer with glaucoma induced by long-term IOP elevation ??. The collagen structure 314 of the peripapillary sclera also became less anisotropic in mouse models of glaucoma?. Computational 315 models have shown that increasing the scleral stiffness relative to the LC stiffness decreases the scleral 316 expansion and increases the posterior displacement of the LC and vice versa. A smaller scleral canal 317 expansion and greater posterior bowing would manifest in inflation tests as a smaller circumferential strain 318 $E_{\theta\theta}$ and larger radial strain E_{rr} in the LC. However, all specimen-averaged normal strain components, 319 including the $E_{\theta\theta}$ and E_{rr} , trended smaller in glaucoma eyes, which suggested that the LC of glaucoma eyes 320 were also stiffer than those of normal eyes. The differences in LC strains were more statistically significant 321 for inflation to 10 mmHg than to 45 mmHg, which suggested that the nonlinear shape of the pressure-strain 322 relationship was different between glaucoma and normal eyes. Inflation studies have also found that the 323 peripapillary sclera of glaucoma human eyes? and experimental monkey eyes? exhibited a stiffer strain 324 response in the low pressure region and a smaller transition stretch marking the strain-stiffening portion of 325 the J-shaped pressure-strain curve. Subsequent finite element modeling studies fit the material parameters 326 of a distributed fiber stress-strain model to the displacement field of the inflation tests and showed that 327 the parameters associated with the collagen crimp and the matrix stiffness tended to be stiffer in glaucoma eyes than normal eyes ??. Sigal and coworkers mapped the collagen crimp in the lamina and cribrosa and 329 peripapillary sclera ?? and showed that the collagen crimp decreased with increased IOP, contributing to the 330 characteristic nonlinear J-shaped, strain-stiffening stress response?. Our findings motivate further studies 331 of the collagen crimp structure in normal and glaucoma eyes. 332

We found larger differences with glaucoma for the normal strains than shear strains. The specimen averaged E_{XY} and $E_{r\theta}$ were near zero for both normal and glaucoma eyes. Differences in the maximum shear strain γ_{max} between normal and glaucoma eyes and between the different damage groups were not significant, and were smaller than for the normal strains and the maximum principal strains. For the normal strains, we also found larger and more significant differences with glaucoma for the nasal-temporal strain E_{XX} than the inferior-superior strain E_{YY} and for the circumferential strain $E_{\theta\theta}$ than the radial strain E_{rr} . That glaucoma affected E_{XX} more significantly than E_{YY} may indicate differences in the anisotropy of the

333

334

335

336

337

339

LC beam structure or in the oval shape of the LC between normal and glaucoma eyes. Gloster? measured a more oval optic cup for glaucoma eyes with visual field defects than for non-glaucoma eyes with full visual fields, and we previously reported larger ratios of E_{XX} and E_{YY} for more oval LCs. The greater differences with glaucoma measured for $E_{\theta\theta}$ than E_{rr} may have been produced by the combined effects of LC and scleral remodeling. Computational models have shown that an increase in the stiffness? and collagen anisotropy? of the peripapillary sclera decrease the scleral canal expansion and increase the posterior LC displacement, while an increase in the LC stiffness decreases the posterior LC displacement. Further studies are needed to investigate the combined effects of alterations in stiffness and anisotropy of the peripapillary sclera and the LC on the different strain outcomes.

The pressure-induced strain response of the LC is also influenced by the thickness and curvature of the LC. The LC of advanced glaucoma eyes with severe optic axon damage are thinner and have a more excavated (cupped) appearance than the LC of normal and early glaucoma eyes ?????. The thinner and more curved LC of glaucoma eyes may explain in part why the LC strains in the more severely damage glaucoma group were larger than those in the more mildly damaged group and why larger differences were measured between peripheral and central LC strains in the more severely damaged glaucoma group. We plan in future studies to estimate the curvature of the LC from 3D reconstruction of the SHG image volumes. After inflation testing, the eyes were fixed and sectioned for more detailed morphological characterization of the collagen structure? These will be analyzed in future work to estimate the thickness of the LC of the inflation tested specimens. Moreover, we are currently developing computational models and an inverse finite element method to estimate the mechanical properties of the LC from the DVC strain fields.

The finding that the LC of more mildly damaged glaucoma eyes tended to be stiffer than for undamaged normal eyes offer two intriguing possibilities. The strain response of the LC of early glaucoma eyes may have been stiffer at baseline, and this may have contributed to the development of glaucomatous axonal damage. Beotra et al. ? reported significantly lower ONH strains *in vivo* in ocular hypertension subjects, who are at higher risk for glaucoma, than healthy subjects for IOP elevation to 30 mmHg, but no difference with glaucoma subjects. Alternatively, the stiffer LC strain response to inflation may have been caused by remodeling of the connective tissue structure and mechanical behavior in early glaucoma. Burgoyne and coworkers have shown using various methods, including *post mortem* histology ? and *in vivo* videography ?

and OCT imaging?, that the posterior displacement response of the ONH of experimental glaucoma monkey 368 eyes became more compliant than the contralateral eye after a couple of weeks of chronic IOP elevation 369 before returning to normal after 13 weeks?. The authors attributed the initial more compliant response 370 to damage of the connective tissue structure of the ONH. The return to a normal displacement response may have been caused by remodeling effects in the early experimental glaucoma monkey eyes, such as 372 thickening of the LC? and increased connective tissue volume fraction?, that stiffen the LC. If the LC were 373 to become more compliant in the initial stage of the human disease, it may have occurred far too early to be 374 detected by the present cross-sectional study of post mortem eyes. Rather, we may have detected in the more 375 mildly damaged glaucoma group the subsequent stiffening effects of remodeling followed by an increase 376 again in compliance in the more severely damaged gluacoma group at a later stage of the disease caused by 377 ONH excavation, LC thinning and widening. Histological studies of glaucomatous human ONH have found alterations in the configuration of elastin?, reorganization of fibril-forming collagens?, and accumulation 379 of s-GAGs and collagen IV in spaces formerly occupied by axons ????. These material remodeling effects 380 would lead to a higher density of collagen, thus result in a stiffer LC stress-strain behavior and smaller LC 381 inflation strains ??, while LC bowing, thinning and widening would promote a more structurally compliant 382 response and larger LC inflation strains with advancing glaucoma damage. 383

We have described the limitations of the inflation method using SHG and DVC in Midgett et al. ?. The more posterior position and more bowed shape of the LC in glaucoma compared to normal eyes made cutting the optic nerve to expose the LC more difficult. The optic nerve section was cut at least 1 mm 386 behind the peripapillary sclera and multiple thin slices were cut from the exposed surface to reveal the LC beams. Despite these precautions, the specimen preparation may have removed part of the LC. However, 388 this would be more likely to occur in the more posteriorly bowed LC of glaucoma eyes, yet we measured smaller strains in these eyes, not the larger strains expected if significant portions of the LC were removed. 390 Moreover, the larger strains that occurred in the moderately to severely damaged glaucoma eyes than in undamaged to mildly damaged eyes, occurred in the peripheral region of the LC rather than the central 392 region that may have been more affected by the specimen preparation. We relied on qualitative evaluation 393 by a glaucoma expert (HQ) of the level of axonal damage in thick sections of the optic nerve of donor eyes. Upon re-examination, the grade of 3 of the nerves changed between the <10% and 10%-25% damage levels,

384

385

387

389

thus we divided the nerves into 2 coarser axon damage levels, a <25% and a >25% axon damage level. 396 Glaucoma eyes with <10% axon damage may have been early in the stage of the disease or misdiagnosed 397 as glaucoma. Recently developed automated axon counting methods may be able to provide a finer grading 398 of axon damage. Automated axon counting methods have been successfully benchmarked against manual 399 axon counting for the optic nerve sections of monkey eyes ?? and rodent eyes ??. For the present study, 400 the quality of axon preservation for some of the human donor eyes, which were received 24-48 hours post 401 mortem, were too poor for accurate axon counts by current automated methods. The sample size was small, 402 with only 6 eyes in the more severe glaucoma damage group and 6-9 eyes in the more mildly damage 403 group, and further studies with a larger number of specimens are needed to confirm the results of a stiffer 404 pressure-strain response in the LC of glaucoma eyes compared to normal eyes. The donor eyes also had 405 different types of glaucoma diagnosis. The majority of the glaucoma donors were diagnosed with POAG, 406 but one donor had ACG, one had pseudoexfoliation glaucoma, and one had an unknown type of glaucoma. 407 The type of glaucoma may also have a strong influence on the LC structure and properties, and separating 408 these effects would require a substantially larger number of specimens. However, further investigations are 409 merited on the basis of these outcomes. 410

5 Conclusions

415

416

417

418

419

420

- We measured the *ex vivo* inflation response of the posterior scleral cup of human donors in the age range of 76-93 years with and without glaucoma and analyzed the pressure-induced LC strains for the effect of glaucoma diagnosis, level of optic nerve damage, and age. The main findings were:
 - LC strains were on average smaller in diagnosed glaucoma eyes compared to age-matched normal
 eyes. The difference in LC strains between the normal and glaucoma groups was larger and more
 statistically significant for inflation to 10 mmHg than to 45mmHg.
 - The LC tensile strains tended to be smaller in the mildly damaged glaucoma group than the undamaged normal group. At 45 mmHg, the tensile strains were also smaller in the mildly damaged glaucoma group than in the severely damaged group. The result were statistically significant for E_{XX} and $E_{\theta\theta}$.

 The more severely damaged eyes had significantly larger peripheral LC strains compared to central LC strains compared to the more mildly damaged glaucoma eyes

These findings suggest that the structural stiffness of the LC were larger in glaucoma eyes than age-matched 423 normal eyes, and was larger at 45 mmHg in more mildly damaged glaucoma eyes compared to undamaged 424 normal eyes and more severely damaged glaucoma eyes. Differences in the structural stiffness of the LC 425 observed in this study may represent both the effects of baseline properties that contribute to axon loss 426 and the effects of remodeling in glaucoma. The lower LC strains in early glaucoma eyes may indicate 427 stiffer baseline properties or connective tissue remodeling in the early disease before significant axon loss. 428 Higher LC strains and larger difference between peripheral and central LC strains in advanced glaucoma 429 eyes may reflect LC thinning, widening, and increased bowing with glaucoma. These findings support the 430 need for further investigations to confirm and quantify differences in the mechanical behavior of the LC with 431 glaucoma, and to study how the LC structure and mechanical behavior are remodeled by glaucoma and how 432 they contribute to the susceptibility and progression of the disease. 433

Disclosures

436

421

422

The authors declare that they have no conflicts of interest.

37 Acknowledgements

- This work was supported by: National Science Foundation (NSF) CAREER Award 1253453, Public Health

 Service (PHS) Research Grants EY021500, EY02120, and EY01765; Brightfocus Foundation grant G2015132;
- National Science Foundation Grant CMMI-1727104; and the Microscopy and Imaging Core Module, Wilmer
- 441 Core Grant for Vision Research. Funding sources and sponsors had no involvement in the design of these
- studies, the collection and analysis of the data, or the writing of this manuscript.